REPORT DOCUMENTATION PAGE	Form Approved OMB NO. 0704-0188

1. REPORT DATE (DD-MM-YYYY)	2. REPORT TYPE	3. DATES COVERED (From - To)
02-09-2011	Conference Proceeding	-

4. TITLE AND SUBTITLE	5a. CONTRACT NUMBER
Fast optically driven spin qubit gates in an InAs quantum dot	W911NF-08-1-0487
	5b. GRANT NUMBER
	5c. PROGRAM ELEMENT NUMBER 411359
6. AUTHORS	5d. PROJECT NUMBER
Erik D. Kim, Katherine Truex, Xiaodong Xu, Bo Sun, D. G. Steel, Allan S. Bracker, Daniel Gammon, Lu Sham	5e. TASK NUMBER
	5f. WORK UNIT NUMBER

7. PERFORMING ORGANIZATION NAMES AND ADDRESSES	8. PERFORMING ORGANIZATION REPORT NUMBER
University of Michigan - Ann Arbor Regents of the University of Michigan 3003 S. State St Ann Arbor, MI 48109 -1274	
9. SPONSORING/MONITORING AGENCY NAME(S) AND ADDRESS(ES)	10. SPONSOR/MONITOR'S ACRONYM(S) ARO
U.S. Army Research Office P.O. Box 12211 Research Triangle Park, NC 27709-2211	11. SPONSOR/MONITOR'S REPORT NUMBER(S) 55014-PH-QC.3

12. DISTRIBUTION AVAILABILITY STATEMENT

Approved for public release; distribution is unlimited.

13. SUPPLEMENTARY NOTES

The views, opinions and/or findings contained in this report are those of the author(s) and should not contrued as an official Department of the Army position, policy or decision, unless so designated by other documentation.

14. ABSTRACT

The ability to manipulate the spin states of charges confined in quantum dots (QDs) is essential for the realization of a quantum computer based on such spins. Here, we present experimentally realized electron spin qubit gates in a single self-assembled InAs QD using a combination of picosecond optical pulses, spin precession about an external DC magnetic field and optically generated geometric phases. Arbitrary unitary operations on the electron spin qubit may be constructed using a combination of optical pulses and either spin precession or the optically generated

15. SUBJECT TERMS

quantum dot; quantum computing; qubit gates; coherent control; spin rotation; geometric phase

16. SECURITY CLASSIFICATION OF:			17. LIMITATION OF ABSTRACT	15. NUMBER OF PAGES	19a. NAME OF RESPONSIBLE PERSON
a. REPORT	b. ABSTRACT	c. THIS PAGE			Duncan Steel
UU	UU	UU	UU		19b. TELEPHONE NUMBER 734-764-4469

Standard Form 298 (Rev 8/98)
Prescribed by ANSI Std. Z39.18

Report Title

Fast optically driven spin qubit gates in an InAs quantum dot

ABSTRACT

The ability to manipulate the spin states of charges confined in quantum dots (QDs) is essential for the realization of a quantum computer based on such spins. Here, we present experimentally realized electron spin qubit gates in a single self-assembled InAs QD using a combination of picosecond optical pulses, spin precession about an external DC magnetic field and optically generated geometric phases. Arbitrary unitary operations on the electron spin qubit may be constructed using a combination of optical pulses and either spin precession or the optically generated geometric phases.

Conference Name: Advances in Photonics of Quantum Computing, Memory, and Communication III

Conference Date: January 28, 2010

Fast optically driven spin qubit gates in an InAs quantum dot

Erik D. Kim[a], Katherine Truex[a], Xiaodong Xu[a], Bo Sun[a], D. G. Steel[a,*], Allan S. Bracker[b], Daniel Gammon[b] and Lu Sham[c]

[a]H. M. Randall Laboratory of Physics, University of Michigan, Ann Arbor, MI 48109, USA
[b]Naval Research Laboratory, Washington D.C. 20375, USA
[c]Department of Physics, University of California, San Diego, La Jolla, CA, 92093-0319, USA

ABSTRACT

The ability to manipulate the spin states of charges confined in quantum dots (QDs) is essential for the realization of a quantum computer based on such spins. Here, we present experimentally realized electron spin qubit gates in a single self-assembled InAs QD using a combination of picosecond optical pulses, spin precession about an external DC magnetic field and optically generated geometric phases. Arbitrary unitary operations on the electron spin qubit may be constructed using a combination of optical pulses and either spin precession or the optically generated geometric phases.

Keywords: quantum dot, quantum computing, qubit gates, coherent control, spin rotation, geometric phase

1. INTRODUCTION

In recent years, the spins of charges confined in semiconductor quantum dots (QDs) have been shown to possess a number of properties attractive for quantum computing implementations[1] due to their three-dimensional confinement.[2,3] These properties include long spin lifetimes[4] and coherence times[5,6] as well as the ability to be grown in scalable patterned structures for device applications.[7,8] Optical approaches to performing quantum computing with QD confined spins have successfully demonstrated spin qubit initialization[9–11] and read-out[11,12] and have recently shown the rotation of such a spin about the optical axis,[13,14] an important step towards the realization of universal quantum gates. Further, optically based spin control allows for the possibility of ultrafast arbitrary single qubit operations,[15] thereby enabling the execution of a large number of operations within the resident spin coherence time.

We present here single qubit gates for an electron spin qubit confined in a single self-assembled InAs QD using optical techniques in conjunction with an external DC magnetic field applied perpendicular to the sample growth axis (Voigt geometry). These gates are based on three different physical processes that rotate the electron spin about a particular axis: pulse-driven two-photon Raman transitions, spin precession about the external magnetic field and optically driven trion Rabi oscillations that impart a geometric phase[16] to one of the electron spin states with each complete cycle. We first investigate the theoretical operation of each process, expressing each operation in terms of a unitary transformation matrix. From these unitary transformation matrices, possible single qubit operations may be determined.

Discussion then turns towards experimental results, beginning with an overview of the sample structure and the experimental setup employed. The sample characterization process is then briefly discussed, followed by a discussion of the general experimental procedure used to demonstrate single spin qubit gates. Experiments are then performed to demonstrate each of the physical processes leading to spin rotation. The results of these experiments are then discussed in detail, as well as possible future directions.

Email: dst@umich.edu

Advances in Photonics of Quantum Computing, Memory, and Communication III, edited by Zameer U. Hasan, Alan E. Craig, Philip R. Hemmer, Charles M. Santori, Proc. of SPIE Vol. 7611, 76110I
 · doi: 10.1117/12.842072

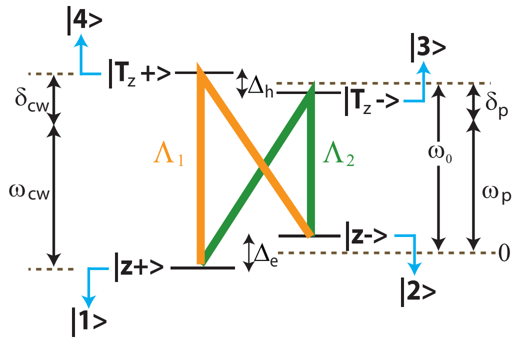

Figure 1. Energy level diagram for the electron spin ground states and the lowest-lying trion states in the presence of an external DC magnetic field along $\hat{z}$. Λ_1 and Λ_2 indicate the two two-photon pathways between the spin ground states. Paramaters for the pulsed and CW optical fields are also indicated. For convenience in theoretical discussions, each state is given a label of the form $|i\rangle$.

2. SINGLE SPIN QUBIT GATES: THEORY

The dynamics of an optically driven QD-confined electron spin in the presence of an externally applied Voigt profile DC magnetic field may be determined by solving for the time-dependent probability amplitudes of the electron spin ground states and the lowest lying trion (negatively charged exciton) states. Fig. 1 illustrates the energy level configuration for a magnetic field applied along the $\hat{z}$ axis, perpendicular to the growth/optical axis $\hat{x}$. For each physical process that leads to spin rotation, we seek the unitary transformation matrix $U(t',t)$ such that

$$\begin{bmatrix} C_1(t') \\ C_2(t') \end{bmatrix} = \begin{bmatrix} & U(t',t) & \end{bmatrix} \begin{bmatrix} C_1(t) \\ C_2(t) \end{bmatrix} \quad (1)$$

where $C_i(t)$ is the probability amplitude associated with state $|i\rangle$ according to the labeling scheme of Fig. 1. The probability amplitudes are determined by solving Schrödinger's equation for the four level system.

2.1 Pulse-Driven Two-Photon Raman Processes

We first consider the operation of an optical pulse highly red-detuned from the electron-trion transitions of the form $\mathbf{E}_p(t) = \frac{1}{2}E_p\text{sech}\left(\frac{t}{\tau}\right)\left[\hat{\epsilon}e^{-i\omega_p t} + c.c.\right]$ with $\hat{\epsilon} = (1/\sqrt{2})(\hat{H} + e^{i\phi}\hat{V})$, where ϕ is an arbitrary phase between the horizontal ($\hat{H}$) and vertical ($\hat{V}$) polarization components. Since the width of pulses employed in experiments ($\sim$ 2 ps) is orders of magnitudes shorter than trion lifetimes measured in these systems,[10] we ignore excited state relaxation and dephasing during the pulse. Further, we assume that the detuning is sufficiently large so as to enable the adiabatic elimination of the trion states. Under these conditions, the unitary transformation associated with the operation of the pulse is found to have the form

$$U_p(\infty,-\infty) = R_x(\theta) = \begin{bmatrix} \cos(\theta/2) & -i\sin(\theta/2) \\ -i\sin(\theta/2) & \cos(\theta/2) \end{bmatrix},\ \theta = \text{Re}\left[ie^{-i\phi}\right]\frac{\Omega_p^2\tau}{\delta_p} \quad (2)$$

where $\Omega_p = (\mu E_p)/\hbar$ is the Rabi frequency associated with the pulse for a trion dipole moment μ, δ_p is the pulse detuning and τ is a measure of the pulse width in time. Employing the notation of Ref.,[17] we find that Eq. 2 has the general form of a counter-clockwise rotation about the optical axis $\hat{x}$ by an angle θ. We also note that the angle of rotation depends on the phase ϕ: for a linearly polarized pulse ($\phi = 0,\ \pi$), $\theta = 0$ and U_p simplifies to the identity matrix, while for a circularly polarized pulse ($\phi = \pm\pi/2$), the absolute value of θ is maximized. Thus, only detuned circularly (or elliptically) polarized pulses are capable of rotating the electron spin, the handedness of the rotation depending on the helicity of the polarization. This polarization dependence may be viewed as a consequence of the interference between the two two-photon quantum pathways (Λ_1 and Λ_2 in Fig. 1) between the electron spin ground states. Useful single qubit gates that may be constructed from Eq. 2 include $R_x(\theta = \pi) = iX$ where X is the Pauli x-matrix and $R_x(\theta = \pi/2) = (2)^{-\frac{1}{2}}(I + iX)$ where I is the identity matrix. The former gate can be used as a single qubit flip gate, while the latter can serve as a component of the important Hadamard gate.

2.2 Spin Precession

Due to the presence of the DC magnetic field along $\hat{z}$, the component of the electron spin vector perpendicular to the magnetic field precesses about $\hat{z}$ at the Zeeman precession frequency Δ_e. The unitary transformation matrix associated with spin precession may be obtained in a straightforward manner and has the form

$$U_{prec}(t,0) = R_z(\vartheta) = \begin{bmatrix} e^{i\vartheta/2} & 0 \\ 0 & e^{-i\vartheta/2} \end{bmatrix},\ \vartheta = \Delta_e t \qquad (3)$$

corresponding to a time-dependent clock-wise rotation about $\hat{z}$. For $\vartheta = \pi$, this rotation performs the operation $R_z(\pi) = iZ$, where Z is the Pauli z-matrix, and can be used as a single qubit "phase flip" gate. Further, this rotation may be used in conjunction with two detuned, time-delayed circularly cross-polarized optical pulses to obtain an effective rotation about the $\hat{y}$ axis, i.e. $R_y(-\vartheta) = R_x(-\pi/2)R_z(\vartheta)R_x(\pi/2)$.

2.3 Optically Generated Geometric Phases

The final method of spin rotation we consider is by the driving of Rabi oscillations in one of the trion transitions with a narrow-bandwidth continuous wave (CW) optical field of the form $\mathbf{E}_{cw} = \hat{V}E_{cw}\cos(\omega_{cw}t)$. For CW Rabi frequencies $\Omega_{cw} = \mu E_{cw}/\hbar$ much greater than the trion relaxation rate, each complete trion Rabi oscillation cycle is essentially a cyclic quantum evolution wherein the wavefunction of the optically driven transition obtains an overall phase Φ. Φ consists of two components: a dynamic component α that depends on the cycle-averaged expectation value of the Hamiltonian and a geometric component β that depends on the geometry of the closed curve representing the cyclic evolution in the particular projective Hilbert space given in Ref.[16]

To determine the forms of the phase components α and β, we consider the case where the $|1\rangle$ to $|4\rangle$ transition is driven by the CW field and take the generalized Rabi frequency $\Omega_g = \sqrt{\Omega_{cw}^2 + \delta_{cw}^2}$ to be sufficiently small so that no other trion transition is driven. In this case, the total phase Φ accrued by the transition wavefunction $|\Psi_{1\to4}\rangle = C_1(t)\,|1\rangle + C_4(t)\,|4\rangle$ for each complete trion Rabi oscillation is $\Phi = \pi\,(1 - \delta_{cw}/\Omega_g)$. Though the dynamic component α of the total phase is generally nonzero, it *is* zero if there is initially no population in the $|4\rangle$ state. Consequently, this is the case encountered in our experiments, since we investigate the operation of the CW field after the operation of a detuned circularly polarized pulse that leaves negligible population in the trion states. Thus, the geometric phase $\beta = \Phi$ and the unitary transformation matrix associated with each complete Rabi oscillation is

$$U_{cw}(T,0) = \mathrm{Ph}(\beta) = \begin{bmatrix} e^{i\beta} & 0 \\ 0 & 1 \end{bmatrix},\ \beta = \pi\left(1 - \frac{\delta_{cw}}{\Omega_g}\right) \qquad (4)$$

where $T = 2\pi/\Omega_g$ is the Rabi period. From Eq. 4, we see that the geometric phase imparted with each CW driven trion Rabi oscillation functions as a general type of phase gate as it alters the phase of the $|1\rangle$ state while leaving the $|2\rangle$ state unaffected. In addition, Eq. 4 may be reexpressed as $\mathrm{Ph}(\beta) = e^{i\beta/2}R_z(\beta)$, signifying that to within a global phase factor $e^{i\beta/2}$, the optically imparted geometric phase effectively rotates the electron spin about the $\hat{z}$ axis by an angle β, the handedness of the rotation depending on the sign of β. It then follows that, in principle, either spin precession or optically imparted geometric phases, which both rotate the spin about $\hat{z}$, may be used with pulse-driven spin rotations about $\hat{x}$ to achieve arbitrary unitary single qubit operations.

3. SAMPLE AND EXPERIMENTAL SETUP

Experiments are performed on a single self-assembled InAs dot contained within in a single-layer QD heterostructure sample grown by molecular beam epitaxy. The sample is placed in a magneto cryostat to enable operating temperatures of approximately 5 K. Optical excitation through 1μm diameter apertures in the Al mask on the sample surface, in conjunction with energy selectivity, enables single QD studies. An external bias voltage provides a means of controlling the number of electrons in a given QD and is set such that the selected dot contains a single electron. Optical pulses are provided by a mode-locked Ti:Sapph laser source that generates pulses ~ 2 ps in width with a repetition period of 13.2 ns while the CW field is provided by a tunable externally-locked Ti:Sapph ring laser with an optical bandwidth of < 500 kHz.

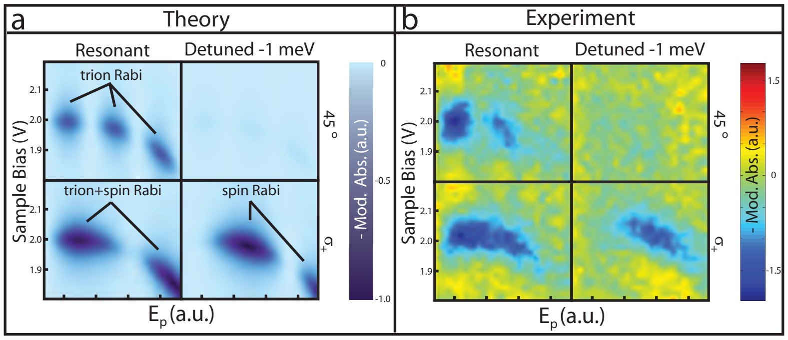

Figure 2. (a) Theoretical and (b) experimentally measured CW absorption signals in one-pulse studies performed with a magnetic field of 5.5 T for different pulse polarizations and detunings as a function of the sample bias voltage and pulse amplitude E_p.

4. QD CHARACTERIZATION

The suitability of a particular dot for experiments is first determined by performing photoluminescence studies to ensure that the emission energies are accessible and sufficiently isolated (by an optical pulse width or more) from those of other nearby QDs. A series of Stark-shift modulation absorption studies[18] are then performed to determine the energies of the trion transitions at different magnetic field strengths. We pay particular attention to the disappearance of the trion absorption signals as the magnetic field is increased as this is a signature of the ability to optically pump the electron spin to a pure state.[10] We employ optical pumping to initialize the spin in the experiments discussed below.

5. EXPERIMENTAL RESULTS

The spin qubit manipulations discussed in Section 2 are experimentally verified by performing a series of experiments where the electron is first initialized by optical pumping, manipulated and then read-out. Specifically, the electron spin is initialized to the $|2\rangle$ state by tuning the CW field to the $|1\rangle$ to $|4\rangle$ transition. Spin manipulation is achieved by exciting the dot with either a single optical pulse train (one-pulse studies) or two time-delayed optical pulse trains (two-pulse studies). Read-out is performed by measuring the time-averaged absorption of the CW field used to initialize the spin in the same manner as with studies used to characterize the trion absorption. Since the combination of pulse delays (if any) and trion lifetimes (~ 1 ns) is much shorter than the pulse repetition period, each pulse (or pulse pair) encounters an initialized spin, thus permitting such time-averaged measurements. Due to spin lifetimes on the order of tens of ms[4] in these systems, absorption measurements in the absence of any spin manipulation yield a negligible signal due to optical pumping. If the operation of the optical pulses results in the generation of population in the $|1\rangle$ state, the optical pumping process is triggered, leading to a measurable absorption signal. This absorption signal provides a means of identifying the different spin control mechanisms and is central to all experiments pursued.

5.1 One-Pulse Studies: Two-Photon Rotations

The first set of experiments performed employs a single pulse train to manipulate the spin after initialization. To uniquely identify the absorption signal resulting from the the driving of two-photon Raman transitions in the dot, experiments are performed comparing the operation of a 45° polarized pulse ($\phi = 0$) with that of a σ_+ polarized pulse ($\phi = \pi/2$) both on resonance and red-detuned approximately 1 meV from the trion transitions. Specifically, CW absorption is measured as a function of the sample bias voltage and the optical pulse amplitude. Figs. 2(a) and (b) plot the theoretically calculated and experimentally observed absorption signals, respectively. Calculations are based on solutions to the density matrix equations for the four level system and include pulse-amplitude dependent red-shift of the trion absorption energy due to pulse-generated carriers in the sample wetting layer and GaAs capping layer. On resonance, both theory and experiment show trion Rabi oscillations for a 45° polarized pulse and a combination of trion and electron spin Rabi oscillations for a σ_+ polarized pulse. Trion

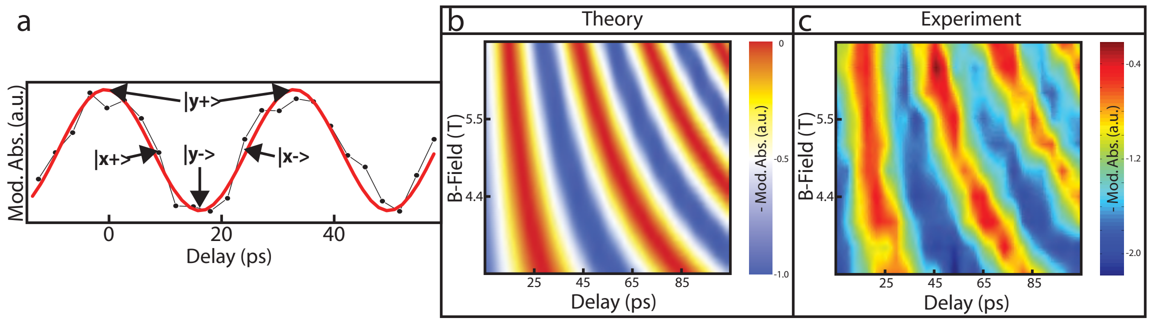

Figure 3. (a) Absorption measurements as a function of pulse delay at 5.5 T. The orientation of the electron spin vector immediately before the second pulse is indicated at selected delays. (b) Theoretically calculated and (c) experimentally measured absorption signals as a function of pulse delay for magnetic field strengths ranging from 3.3 T to 6.6 T.

Rabi oscillations are observed due to the fact that any trion population generated by the pulses decays to either electron spin ground state with nearly equal probability, resulting in non-negligible absorption signal. For a σ_+ polarized pulse, a complete spin flip ($\theta = \pi$) occurs when the amount of trion population generated is minimal.

By detuning the pulses, the amount of trion population generated may be suppressed without affecting the trion Rabi frequency. This leads to an almost negligible absorption signal for 45° polarization. For the two-photon Raman processes, detuning decreases the spin Rabi frequency but does not suppress the absorption signal resulting from the two-photon rotations. Thus, the absorption signal observed for σ_+ polarization is due entirely to the driving of two-photon Raman processes. The right columns of Fig. 2(a) and (b) verify this general behavior in both theory and experiment, though experimental results show a full rotation of the spin while the theory shows slightly beyond a full rotation. The reasons for the discrepancy between the theoretical and experimentally observed spin Rabi frequencies are not clear currently, though one possible cause may be birefringence in the sample layers above the QD, which would lead to elliptically polarized pulses at the dot. Elliptical polarization would correspond to a ϕ value different from $\pi/2$, leading to a reduced magnitude of θ and, hence, a reduced spin Rabi frequency. Nevertheless, a detuned circularly polarized pulse may be used to execute spin rotations about the optical axis $\hat{x}$ on timescales determined by the pulse width and with fidelities approaching unity as the detuning is increased. The spin qubit gates $R_x(\pi)$ and $R_x(\pi/2)$ mentioned in Section 2.1 may be realized by setting the pulse amplitude to the value that yields the maximum absorption signal and the first value that yields one half the maximum absorption signal, respectively.

5.2 Two-Pulse Studies: Spin Precession

Having demonstrated the use of detuned circularly polarized pulses to rotate the spin about the optical axis, we now turn to studies using two red-detuned, time-delayed σ_+ polarized pulses of pulse area $\theta = \pi/2$. These studies enable the observation of transient phenomena that occur between pulses and are first used to observe spin precession. Since the CW initialization field is constantly left on, we consider pulse delays much shorter than the CW Rabi period T to focus on the effect of spin precession on the measured absorption signal.

In these experiments, the first $\pi/2$ pulse rotates the electron spin vector into the plane perpendicular to the magnetic field. Due to precession, the final projection of the spin vector along the magnetic field axis after the second pulse, which determines the measured absorption signal, depends on the time delay between the two pulses. Thus, absorption measurements as a function of pulse delay will oscillate at the electron Zeemen splitting frequency Δ_e. This oscillatory dependence is clearly exhibited in Fig. 3(a), which plots absorption measurements as a function of pulse delay for an external magnetic field of 5.5 T. To further confirm the observation of spin quantum beats, we perform these absorption measurements for magnetic field strengths ranging from 3.3 T to 6.6 T. Figs. 3(b) and (c) plot the theoretically calculated and experimentally measured absorption signals as a function of pulse delay, both showing the expected dependence of the precession frequency on the magnetic field strength. From the oscillation frequency, an electron g-factor magnitude of 0.4 is extracted. From the data, we see that at higher magnetic field values, complete rotations about the magnetic field axis $\hat{z}$ may be obtained within a few tens of ps. The operation of the two $\pi/2$ pulses and spin precession constitutes a composite gate

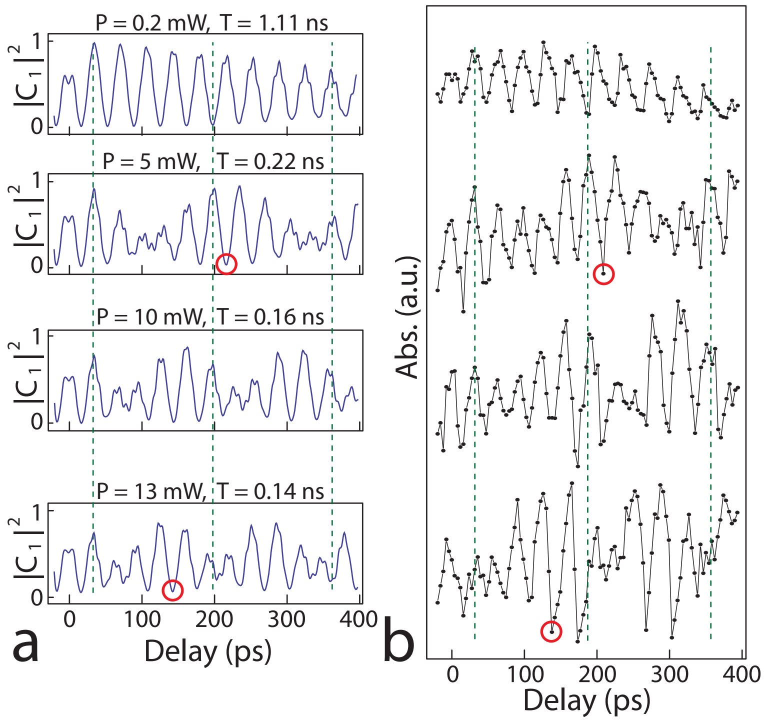

Figure 4. (a) Theoretically calculated values of the $|1\rangle$ state population immediately after the second pulse and (b) the corresponding experimentally measured absorption measurements as a function of pulse delay for different CW field powers and a magnetic field of 5.5 T. The effect of the optically imparted geometric phases may be observed by comparing the scans at the delays indicated by the green dashed lines. Red circles indicate the cases where the trion Rabi period is roughly equal to an integer number of spin precession periods, enabling the construction of purely optical spin manipulations.

of the form $i[\sin(\vartheta/2)Z - \cos(\vartheta/2)X]$. To within a leading phase term, a composite Z operation is obtained at $\vartheta = \Delta_e t = \pi$.

5.3 Two-Pulse Studies: Optically Generated Geometric Phases

As mentioned in the previous section, the CW initialization field is left on between pulses and thus drives Rabi oscillations between the $|1\rangle$ and $|4\rangle$ states as the electron spin precesses and is re-initialized. If two-pulse studies are repeated covering delay ranges comparable to or greater than the CW Rabi period, the effect of CW driven trion Rabi oscillations may be observed in the measured absorption signal. Since the CW field resonantly drives the $|1\rangle$ to $|4\rangle$ transition, $\Omega_g = \Omega_{cw}$ and $\Phi = \beta = \pi$. As a result, two additional features in the spin quantum beat signal are expected: 1) a modulation envelope of frequency Ω_{cw} and 2) a phase shift of π in the quantum beat signal with each complete trion Rabi oscillation. The modulation envelope is a result of the CW field driving population from $|1\rangle$ to $|4\rangle$ during each trion Rabi oscillation: at times when the $|4\rangle$ population is maximized, the electron spin vector lies along the magnetic field axis (i.e. along $-\hat{z}$) and does not precess, resulting in a quantum beat amplitude of zero.

Fig. 4 plots (a) the theoretically calculated values of the $|1\rangle$ population immediately after the second $\pi/2$ pulse and (b) the corresponding experimentally measured absorption signals for longer delay ranges and different CW field powers. Both theory and experiment clearly show a CW power dependent modulation of the spin quantum beat signal. Further, comparison of the absorption scans at delays indicated by the dashed green lines enable observation of the geometric phase imparted to the $|1\rangle$ state with each complete trion Rabi oscillation. Near zero delay, all quantum beat signals start initially in phase. Around 200 ps, the 5 mW and 10 mW absorption scans, which have each undergone roughly a complete trion Rabi oscillation, are π out of phase with the .2 mW scan, which does not undergo a complete trion Rabi oscillation in the delay range covered. The 13 mW absorption scan shows a phase shift of less than π since it is approaching a $|1\rangle$ population depletion point, near which the phase changes rapidly. After undergoing a second complete trion Rabi oscillation (near 350 ps), the 5 mW and 10 mW scans are once again in phase with the .2 mW scan, each having undergone two π phase shifts. This result demonstrates the ability to control the total geometric phase acquired by the $|1\rangle$ state by driving multiple trion Rabi oscillations. Arbitrary phase shifts may in principle be obtained using a combination of different CW field detunings and multiple trion Rabi oscillations, the speed of operation determined by the Rabi period T.

We note further that entirely optically driven arbitrary spin rotations may be constructed from a combination of pulse-driven rotations and optically imparted geometric phases when the trion Rabi period is equal to an integer multiple of spin precession periods. Cases where this condition is approximately met in experiments with a resonant CW field are indicated by the red circles in Fig. 4. At those points, the total operation of the two $\pi/2$ pulses and the CW-driven trion Rabi oscillation, to within a leading phase term, forms an optically driven composite Z gate.

6. CONCLUSIONS AND FUTURE DIRECTIONS

We have investigated single qubit gates for an electron spin confined in a self-assembled InAs QD in both theory and experiment for three different physical processes that rotate the spin: pulse-driven two-photon Raman transitions, spin precession and optically generated geometric phases. Mathematical expressions for the operation of each process were obtained in terms of unitary transformation matrices, from which possible single qubit gates may be determined. Experiments utilizing pulsed and CW optical fields in conjunction with an externally applied DC magnetic field in the Voigt geometry were performed to demonstrate particular spin qubit gates executed by each of the physical processes.

To more rigorously demonstrate the execution of single qubit gates presented here and evaluate their fidelities, density matrix tomography may be performed to map out the system density matrix elements using the combination of a detuned circularly polarized optical pulse and spin precession. Such a procedure would require a careful characterization of the fidelities of the rotations performed by the pulses and spin precession, though such a procedure should in principle be straightforward to develop given the results presented here.

In addition, the use of optically generated geometric phases to control the electron spin demonstrated here may be developed further to enable the use of optical pulses to impart equal and opposite geometric phases to the resident spin states as proposed in Ref.[15] This could potentially allow operation times on the order a few tens of ps, an order of magnitude shorter than the shortest operation time of $\sim$ 140 ps obtained here with a 13 mW CW field (Fig. 4).

This work was supported in part by ARO/LPS/IARPA, AFOSR, DARPA, NSF, and ONR.

REFERENCES

1. D. P. DiVincenzo, “The Physical Implementation of Quantum Computation”, *Fortschr. Phys.* **48**, 771 (2000)
2. A. Imamoğlu, D. D. Awschalom, G. Burkard, D. P. DiVincenzo, D. Loss, M. Sherwin and A. Small, “Quantum information processing using quantum dot spins and cavity QED”, *Phys. Rev. Lett.*, **83**, 4204 (1999)
3. D. Loss and D. P. Di Vincenzo, “Quantum computation with quantum dots”, *Phys. Rev. A*,**57**, 120 (1998)
4. M. Kroutvar, Y. Ducommun, D. Heiss, M. Bichler, D. Schuh, G. Abstreiter and J. J. Finley, “Optically programmable electron spin memory using semiconductor quantum dots”, *Nature*, **432**, 81 (2004)
5. D. Brunner, B. D. Gerardot, P. A. Dalgarno, G. Wüst, K. Karrai, N. G. Stoltz, P. M. Petroff and R. J. Warborton, “A Coherent Single-Hole Spin in a Semiconductor”, *Science*, **325**, 70 (2009)
6. X. Xu, W. Yao, B. Sun, D. G. Steel, A. S. Bracker, D. Gammon and L. J. Sham, “Optically controlled locking of the nuclear field via coherent dark-state spectroscopy”, *Nature*, **459**, 1105 (2009)
7. G. Springholz, V. Holy, M. Pinczolits and G. Bauer, “Self-Organized Growth of Three-Dimensional Quantum-Dot Crystals with fcc-Like Stacking and a Tunable Lattice Constant”, *Science*, **282**, 734 (1998)
8. H. Lee, J. A. Johnson, M. Y. He, J. S. Speck, P. M. Petroff, “Strain-engineered self-assembled semiconductor quantum dot lattices”, *Appl. Phys. Lett.*, **78**, 105 (2001)
9. M. Atatüre, J. Dreiser, A. Badolato, A. Högele, K. Karrai and A. Imamoğlu, “Quantum-Dot Spin-State Preparation with Near-Unity Fidelity”, *Science*, **310**, 551 (2006)

10. X. Xu, Y. Wu, B. Sun, Q. Huang, J. Cheng, D.G. Steel, A.S. Bracker, D. Gammon, C. Emary and L.J. Sham, "Fast spin state initialization in a singly charged InAs-GaAs quantum dot by optical cooling", *Phys. Rev. Lett.*, **99**, 097401 (2007)
11. D. Kim, S. E. Economou, S. C. Badescu, M. Scheibner, A. S. Bracker, M. Bashkansky, T. L. Reinecke and D. Gammon, "Optical Spin Initialization and Nondestructive Measurement in a Quantum Dot Molecule", *Phys. Rev. Lett.*, **101**, 236804 (2008)
12. J. Berezovsky, M. H. Mikkelsen, O. Gywat, N. G. Stoltz, L. A. Coldren and D. D. Awschalom, "Nondestructive Optical Measurements of a Single Electron Spin in a Quantum Dot", *Science*, **314**, 1916 (2006)
13. J. Berezovsky, M. H. Mikkelsen, N. G. Stoltz, L. A. Coldren and D. D. Awschalom, "Picosecond Coherent Optical Manipulation of a Single Electron Spin in a Quantum Dot", *Science*, **320**, 349 (2008)
14. D. Press, T. D. Ladd, B. Zhang and Y. Yamamoto, "Complete quantum control of a single quantum dot spin using ultrafast optical pulses", *Nature*, **456**, 218 (2008)
15. S. E. Economou and T. L. Reinecke, "Theory of Fast Optical Spin Rotation in a Quantum Dot Based on Geometric Phases and Trapped States", *Phys. Rev. Lett.*, **99**, 217401 (2007)
16. Y. Aharonov and J. Anandan, "Phase Change during a Cyclic Quantum Evolution", *Phys. Rev. Lett.*, **58**, 1593 (1987)
17. M. A. Nielsen and I. L. Chuang, *Quantum Computation and Quantum Information*, First Edition, Cambridge University Press, Cambridge, United Kingdom, 2000
18. B. Alen, F. Bickel, K. Karrai, R. J. Warburton and P. M. Petroff, "Stark-shift modulation absorption spectroscopy of single quantum dots", *Appl. Phys. Lett.*, **83**, 2235 (2003)